Journal of Materials Science and Chemical Engineering, 2023, 11, 34-45
https://www.scirp.org/journal/msce
ISSN Online: 2327-6053
ISSN Print: 2327-6045

Formulation of Geopolymer Cements from Two Clays Containing Kaolinite and Muscovite: Effect of Temperature on the Physicomechanical Properties of the Products

Mamadou Yaya Balde[1,2,3*], Diaka Sidibe[4], Éric Severin Simo Bakam[1], Chantale Djangang Njiomou[1], Philippe Blanchart[5]

[1]Laboratory of Applied Inorganic Chemistry, University of Yaoundé 1, Yaoundé, Cameroon
[2]Laboratory of Physical and Colloidal Chemistry, Gamal Abdel Nasser University of Conakry, Conakry, Guinée
[3]Center for Waste Management Research (CREGED), Conakry, Guinea
[4]Higher Institute of Mines and Geology of Boké (ISMGB), Boké, Guinea
[5]Institute of Research for Ceramics (IRCER), Limoges, France
Email: *baldez201073@gmail.com

How to cite this paper: Balde, M.Y., Sidibe, D., Simo Bakam, É.S., Djangang Njiomou, C. and Blanchart, P. (2023) Formulation of Geopolymer Cements from Two Clays Containing Kaolinite and Muscovite: Effect of Temperature on the Physicomechanical Properties of the Products. *Journal of Materials Science and Chemical Engineering*, **11**, 34-45.
https://doi.org/10.4236/msce.2023.1112004

Received: November 24, 2023
Accepted: December 26, 2023
Published: December 29, 2023

Abstract

The paper talks about the elaboration of geopolymer with two types of kaolinite clays containing muscovite. The kaolinite materials were first calcined at different temperatures, and mixed with an activator solution, called liquid precursor, at a different solid/liquid mass ratio depending on their normal consistency to produce geopolymer binders. Results show that the geopolymer products obtained from the different clays have good physichomechanical properties: their open porosity and their water absorption rate decrease while their compressive strength and their apparent density increase with the increase in calcination temperature of the clays. The density of GABD binders varies between 2.92 and 2.47 g/cm^3 and that of GARD binders between 1.86 and 2.16 g/cm^3. Specimens in the GABD series have the best mechanical performance, ranging from 14.43 to 31.37 MPa, while those in the GARD series oscillate between 6.18 and 11.56 MPa. These properties make kaolinite materials from this region suitable for use as construction materials for adequate waterproof structures.

Keywords

Geopolymer Cements, Kaolinitic Clays, Muscovite, Permeability, Mechanical Strength

1. Introduction

Hydraulic cement, also known as conventional cement, is a material used as a binder in concrete and mortar-based structures. It is a key element in modern construction worldwide [1] [2]. Its main component is clinker, the production of which not only requires a lot of energy, but also significantly emits carbon dioxide, a greenhouse gas. These gases contribute to ozone layer depletion and global warming, which have become global concerns [2] [3] [4] [5] [6]. Furthermore, the increasing cost of Portland cement in our markets has become a pressing issue, making modern construction unaffordable for many, despite the inadequate housing conditions in our society. In this context, the development of a binder with reduced carbon footprint and greater accessibility for all can be a sustainable solution to the aforementioned problems. Geopolymer binders are among the most recent and promising alternatives to cement, aiming at reducing energy consumption and greenhouse gas emissions [5] [7]. They are the counterparts of organic polymers resulting from the consolidation of natural or synthetic aluminosilicates at ambient or low temperatures in highly alkaline environments, forming highly resistant chemical structures that can withstand external aggressions and even fire [8] [9] [10] [11]. The raw materials commonly used for geopolymer synthesis vary, including industrial by-products, volcanic slags, and kaolinitic or halloysitic clays. These raw materials often contain various clay and non-clay minerals. Understanding the influence of associated minerals on geopolymers' formation is of interest for mastering the consolidation process. The present study aims to investigate the role of muscovite in the geopolymerization involving a muscovite-rich kaolinite.

2. Materials and Methods

2.1. Materials

The two clays (**Figure 1**) used in this study come from Débélé, Kindia prefecture (Republic of Guinea). They are respectively named ABD and ARD based on their color; the former being white and the latter reddish in color [12].

The physicochemical and mineralogical characterization of the samples, previously determined, is presented in **Table 1** [12] [13]. Thus, the illustrations relating to these analyses: XRD, thermal analysis, and Fourier transform infrared will not be presented in this work [12].

Figure 1. Appearance of raw clay samples from the Débélé locality (Kindia, Guinea).

Table 1. Physicochemical and mineralogical characteristics of the clays [12].

Components	*ABD*	*ARD*
Physical parameters		
Bulk density (g/cm^3)	2.4	2.5
Specific surface area (m^2/g)	42.2	23.3
Plasticity index	25	23
Clay phase: 2 < Φ < 20 µm	51.6	48.5
Clay phase: Φ < 2 µm (%)	48.5	51.0
Chemical composition		
SiO_2	52.40	51.20
Al_2O_3	30.90	30.40
Fe_2O_3	1.80	3.70
K_2O	5.90	4.80
TiO_2	1.60	1.60
MgO	0.50	0.40
CaO	0.10	0.10
Na_2O	0.20	0.10
P_2O_5	0.10	0.10
Cr_2O_3	0.02	0.02
SO_3	0.13	0.030
MnO	<0.01	<0.01
LOI	6.20	7.50
Total	99.74	99.96
Mineralogical composition (%)		
Kaolinite	57.4	55.1
Muscovite	27.0	19.9
Quartz	11.3	18.3
Hematite	1.8	/
Anatase	1.6	1.6
Gibbsite	0.6	0.5
Goethite	/	4.6
Total	99.70	100.00

2.2. Methods

The chemical composition (XRF) and mineralogical composition (XRD, differential thermal analysis) were previously determined [12].

To make the materials more reactive, the powders constituting the clay frac-

tion were thermally treated in a Nabertherm LH 60/14 electric furnace at temperatures of 600˚C, 700˚C, and 800˚C. The activating solution was obtained by equimolar mixing of a commercial sodium silicate solution (INGESSIL) with mass proportions of SiO_2 (28.7%), Na_2O (8.9%), and H_2O (62.4%) with a sodium hydroxide solution (8 M) obtained by dissolving flakes of this salt (CAMEO Chemicals) in distilled water, with a purity of 99%. For each of the two solid precursors, the geopolymer binder was prepared by mixing the aluminosilicate powder (solid precursor) with the activating solution (liquid precursor) in a solid/liquid (S/L) mass ratio of 1.20 for ABD and 1.11 for ARD, as shown in Table 2.

Indeed, these ratios were selected as those that provided the best consistency following multiple trials. The mixture was homogenized using an M&O brand mixer, model N50-G, for a duration of ten minutes. The viscous paste obtained is used for shaping the experimental specimens and for determining the initial and final setting times. Regarding the shaping of the specimens, the paste is poured into cylindrical PVC molds (diameter = 20 mm, height = 40 mm). To prevent early water evaporation during the setting and hardening of the paste, the specimens are covered with a thin film of polyethylene and placed in the laboratory's ambient atmosphere (24˚C ± 3˚C). Demolding is carried out 24 and 48 hours after casting, respectively for ARD and ABD. After demolding, physical measurements are performed according to ISO 5017/1985 standard based on the Archimedes test (ISO Standard, 2013). The implementation involves drying the geopolymer specimen pellets in an oven at 105˚C, allowing them to cool completely in a desiccator, and measuring their mass (M_1). Then, they are immersed in distilled water contained in a crystallizing dish, and the ensemble is placed in a vacuum-sealed chamber (pressure of 150 mBar) to allow water saturation. The apparent mass (M_2) of the specimen is determined when it is submerged in water, with the ensemble suspended from a balance beam. Afterwards, the specimen is removed from water, quickly freed from droplets and surface water film using an absorbent cloth, and immediately weighed to obtain its mass in air (M_3) [14]. The tests were conducted on five pellets of each formulation, and the desired quantity is obtained by taking the average of consistent values. The apparent density ρ is given by *Equation* (1):

Table 2. Types of formulations for geopolymer binder mixes.

Formulations	% aluminosilicate	% solution alcaline	S/L ratio
GABD 600	54.55%	45.45%	1.20
GABD 700	54.55%	45.45%	1.20
GABD 800	54.55%	45.45%	1.20
GARD 600	52.53%	47.47%	1.11
GARD 700	52.53%	47.47%	1.11
GARD 800	52.53%	47.47%	1.11

$$\rho = \frac{M_1}{M_3 - M_2} \times \rho_{eau} \quad (1)$$

where ρ_{eau} (g/cm^3) is the density of water at the temperature of the experiment.

The open porosity, Π, expressed as a mass percentage (%), is given by *Equation* (2):

$$\pi = \frac{M_3 - M_1}{M_3 - M_2} \times 100 \quad (2)$$

The water absorption rate, W, is given by *Equation* (3):

$$W = \frac{M_3 - M_1}{M_1} \times 100 \quad (3)$$

The compressive strength (δ) is measured according to the EN 196-1 standard. It is carried out on geopolymer test specimens aged 14, 28, and 42 days, maintained at the laboratory's room temperature. The principle involves placing the specimen on the platen of an electrohydraulic press manufactured by Impact Test Equipment Limited, with a capacity of 250 KN. Subsequently, it is subjected to a continuous and progressive load at an average rate of 0.5 MPa/s until failure. The compressive strength is the ratio of the maximum load (F) sustained by the specimen during the test to the cross-sectional area(s) of the tested specimen, as per *Equation* (4):

$$\delta = \frac{4 * 10^3 * F}{\pi D^2} \quad (4)$$

where F is the crushing force of the specimen in Kilo Newtons (KN); D is its diameter in meters (mm) and δ is the strength in Mega Pascal (MPa).

At each age of the specimen, the retained strength is the average of consistent results from five conducted tests.

3. Results and Discussion

3.1. Physicochemistry of Precursors

Regarding the chemical composition of the starting clay materials ABD and ARD (**Table 1**), it can be observed that silica (SiO_2) and alumina (Al_2O_3) are the major oxides. Furthermore, ABD contains slightly more silica and alumina than ARD, although the molar ratio of SiO_2/Al_2O_3 is the same in both cases, equal to 2.9. It should be noted that these two oxides are crucial for the reactivity of solid precursors, hence the term "aluminosilicate precursors," as they initiate the geopolymerization mechanism [12] [15]. Considering the alkali oxides, the content is low for Na_2O (0.16% in ABD and 0.09% in ARD) compared to K_2O (5.88% in ABD and 4.78% in ARD), indicating the presence of mica minerals in both materials [16] [17] [18]. The alkaline-earth oxides (CaO and MgO) are present in small percentages. As for the coloring oxides, the content of TiO_2 is practically the same in both materials (1.62% for ABD and 1.61% for ARD), while the content of Fe_2O_3 is higher in ARD (3.65%) than in ABD (1.77%). The main clay minerals present in both materials (**Table 1**) are kaolinite ($Al_2Si_2O_5(OH)_4$) and

muscovite ($KAl_2(Si_3Al)O_{10}(OH,F)_2$). Non-clay minerals such as quartz (SiO_2), anatase (TiO_2), gibbsite ($Al(OH)_3$), hematite (Fe_2O_3), and goethite (FeO(OH)) are present in minor quantities [12].

The quantities of amorphous phases at different temperatures of aluminosilicate precursors are recorded in **Table 2**. A strong increase in the percentage of amorphous phase is observed with the calcination temperature. This allows for optimizing the properties of synthetic products since materials with a higher amorphous phase content exhibit greater reactivity [19]. Similarly, in the presence of alkaline solution, the amorphous phases dissolve more easily during the initial geopolymerization step to produce the main monomer species $[SiO(OH)_3]^-$ and $[Al(OH)_4]^-$. These percentages remain high for ABD materials compared to those of the ARD type, which suggests better mechanical properties for GABD-type geopolymers. This brings us to consider the role of muscovite, whose content truly makes a difference between the two starting materials and consequently the derived precursors.

3.2. Physicomechanical Properties of Geopolymer Binders

The appearance of geopolymer binder specimens at demolding and at the 42nd day is illustrated in **Figure 2**. These specimens are characterized by the absence of any surface defects, such as efflorescence, which is a common phenomenon in aluminosilicate-based geopolymers [20] [21].

The absence of efflorescence is due to the rapid dissolution rate which prevents the infiltration of CO_2 from the air into the geopolymer matrix. Furthermore, the specimens maintained their shape from demolding until the testing periods, indicating good consolidation and sealing, confirming their stability over time.

This stability is also demonstrated by the evolution of open porosity and water absorption rate in the geopolymer binders as a function of age. A progressive

Table 3. Quantities of amorphous phases as a function of temperature.

Materials	Treatment temperature (˚C)			
	25	600	700	800
ABD	34.6	71.9	73.5	76.5
ARD	29.9	63.5	65.5	70.2

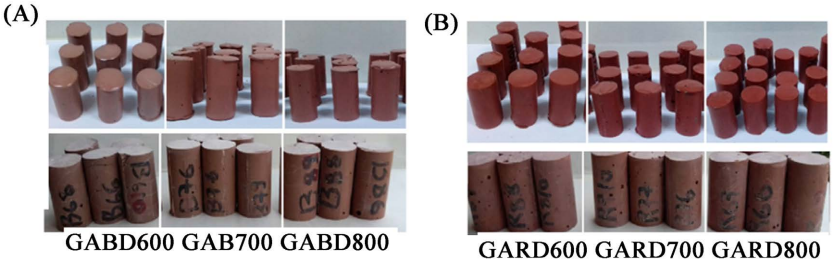

Figure 2. Appearance of the geopolymers specimens.

decrease in these two parameters is observed, not only with age but also with the activation temperature of the precursors in each series (**Figure 3(A)** and **Figure 3(B)**). However, the values of open porosity remain significant for GARD specimens (**Figure 3(Ab)**), decreasing from 44.40% to 38.15% from 600˚C to 800˚C precursor temperature on the 14th day, compared to only 12.73% to 8.96% for GABD specimens (**Figure 3(Aa)**). The same observation was made on the 42nd day, where porosity decreased from 37.49% to 35.41% for GARD and from 8.96% to 6.91% for GABD.

The decrease in pore density of the geopolymer product is correlated with the observed decrease in absorption rate (**Figure 3(B)**). It should be noted that these two parameters are interrelated, as they are characteristic of the permeability and durability of the product. Indeed, on the 42nd day, the variation in absorption rate depending on the precursor obtaining temperature ranges from 19.63% to 18.74% for GARD and from 3.86% to 2.84% for GABD. The muscovite present in the starting clays, depending on its content, contributed to the reduction of the viscosity of the geopolymeric gel, resulting in hardening with the arrangement and aggregation of oligomers that ensure the closure of pores, leading to a decrease in accessible pore volume. As previously mentioned, during its thermal treatment around 700˚C, muscovite promotes the formation of a less viscous flux with increasing calcination temperature and its content [22]. Moreover, it is

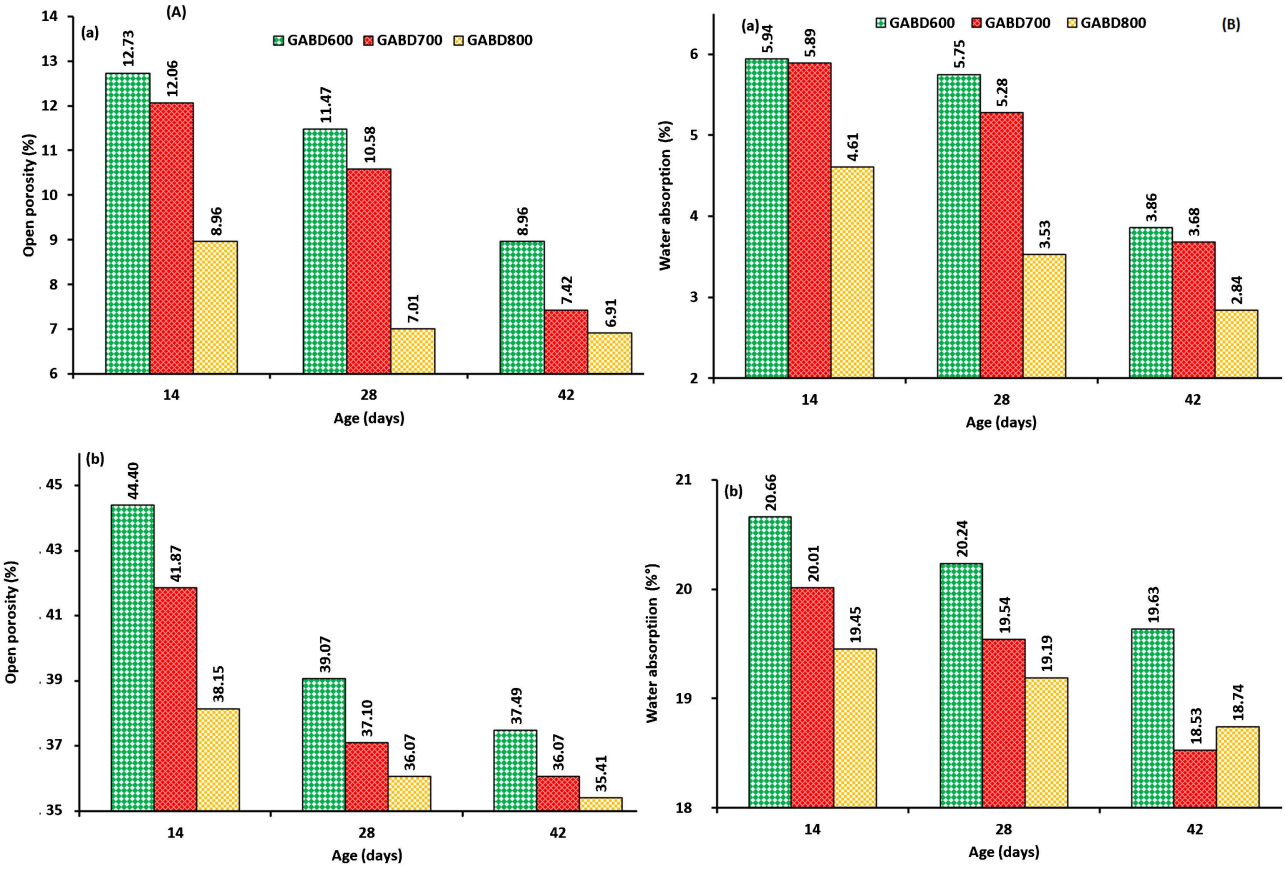

Figure 3. Evolution of open porosity (A) and water absorption rate (B) of the specimens.

argued that excessively high values of these parameters promote interactions with the external environment, and for structural-type applications where impermeability is required, it is desirable to have low permeability [23]. This means that low porosity and subsequent low absorption rate lead to appreciable performances. Not forgetting the effect of thermal activation of precursors, these performances are reflected in the development of apparent density and compressive strength (**Figure 4(A)** and **Figure 4(B)**) of the obtained binders, which increase with the age of the specimens. The density of GABD type binders varies in the range of 2.92 to 2.47 g/cm^3, while that of GARD type varies between 1.86 and 2.16 g/cm^3. Consequently, the products are denser in the former case than in the latter. Indeed, the geopolymerization process is more intense in the ABD-based formulations containing higher proportions of kaolinite and muscovite (**Table 3**). This means that these minerals have contributed favorably to the densification and development of mechanical performances (**Figure 4(B)**), as predicted by some authors [24] [25]. The specimens in the GABD series have the best mechanical performances, ranging from 14.43 to 31.37 MPa, while those in the GARD series range from 6.18 to 11.56 MPa.

In summary, the amorphous phase content and thermal transformation of muscovite as a fluxing mineral have played a significantly favorable role in the development of mechanical strengths, as demonstrated by the works of Yang *et al.* [26].

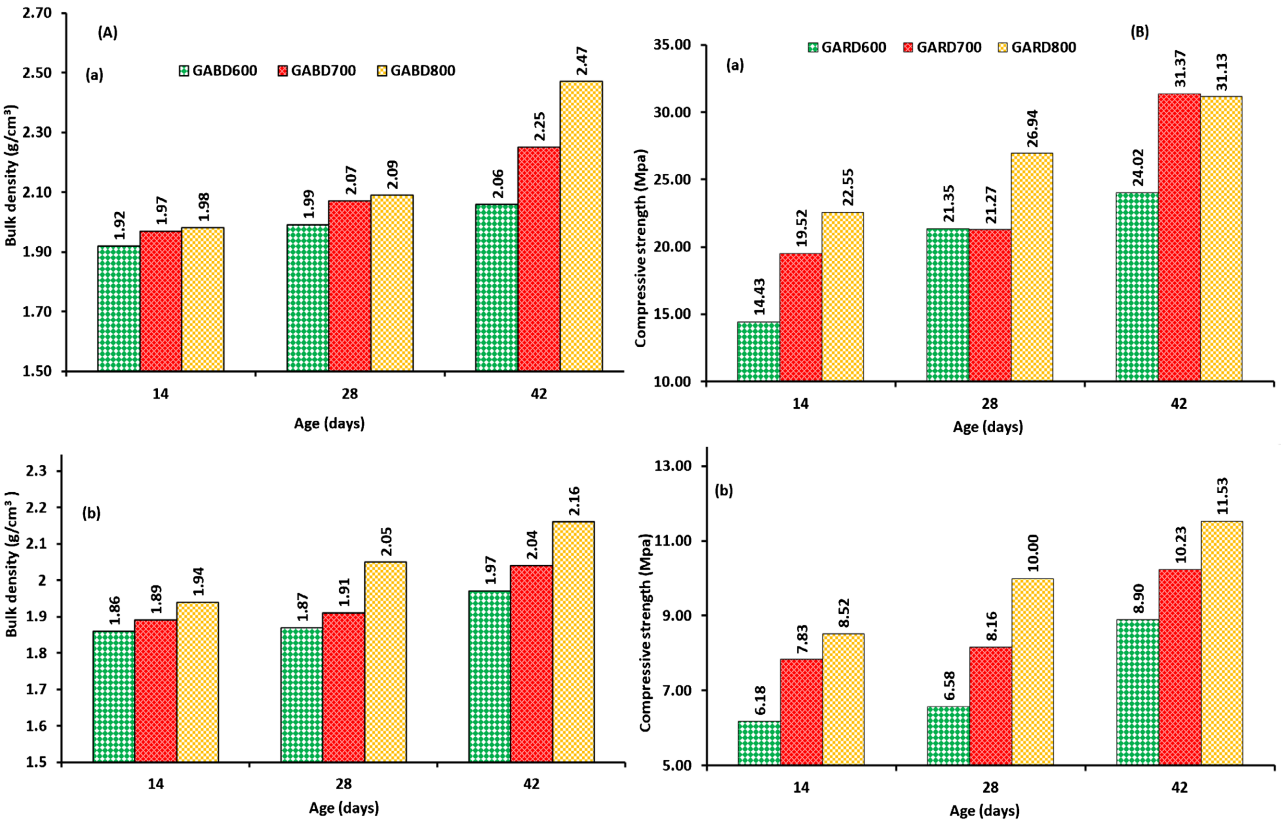

Figure 4. Apparent density (A) and compressive strength (B) as a function of age for specimens of (a) GABD and (b) GARD.

3.3. Microstructural Properties of Geopolymer Binders

The formation of the geopolymer gel based on the two precursors used resulted in a microstructure that could be observed by optical microscopy (**Figure 5**).

The micrographs of different geopolymer binders obtained by optical microscopy are illustrated in **Figure 5**. Generally, the binders have a more or less homogeneous microstructure with a slight difference in particle connectivity within the matrix. In the case of GABD samples, a structure scattered with whitish particles can be observed, which some authors have attributed to the residual phase linked to either the liquid precursor or additives [26] [27] [28] [29].

For the GARD samples, macropores appear on the matrix surface. This observation correlates with the very high open porosity (35.41% to 44.40% pores) discussed earlier (**Figure 3**) [30] [31] [32]. Ultimately, the products from the GABD series are characterized by a densely connected three-dimensional network microstructure, consistent with their high bulk density values. The low permeability and high mechanical performance compared to the GARD series, whose clay precursor contains less muscovite, confirm the densification role of this mineral.

Figure 5. Optical microscopy images of the geopolymers.

4. Conclusions

The aim of this work was to experiment with the application of two varieties of clay from Débélé (Guinea) in the composition of hydraulic binders with a view to their recovery. The two kaolinitic clays, ABD and ARD, were calcined at temperatures of 600˚C, 700˚C and 800˚C respectively to obtain aluminosilicate precursors that were used in the formulation of geopolymer binders. The binders were formulated by mixing the above-mentioned solid aluminosilicate precursors and the liquid precursor or activating solution in a solid/liquid mass ratio of 1.20 for the ABD precursors and 1.11 for the ARD precursors. The products were characterised in terms of their physical appearance, physicomechanical properties and structural (FTIR) and microstructural (optical microscopy) phases.

The results show that:

- Aluminosilicate precursors have a proportion of amorphous phases, which naturally increases with the amorphisation temperature of the clays;
- Specimens of the binders obtained show good consolidation from demoulding and continue with age;
- On day 42 and depending on the activation temperature, the specimens have densities of between 2.06 and 2.47 g/cm^3 for GABD and between 1.97 and 2.16 g/cm^3 for GARD, as a result of the gradual reduction in open porosity and the rate of water absorption.

These products can, therefore, be used as construction materials for structures where waterproofing is required, mainly in cases where the muscovite content is high in the starting clay. However, structural studies using XRD and microstructural studies using SEM could be envisaged to better guide the use of the products obtained.

Acknowledgements

The authors would like to thank the authorities of the Ministry of Higher Education, Scientific Research and Innovation of Guinea and the Faculty of Science of the University of Yaoundé 1.

Conflicts of Interest

The authors declare no conflicts of interest regarding the publication of this paper.

References

[1] Van Oss, H.G. and Padovani, A.C. (2002) Cement and the Environment: Part I: Chemistry and Technology. *Journal of Industrial Ecology*, **6**, 89-105. https://doi.org/10.1162/108819802320971650

[2] Özen, S. and Alam, B. (2018) Compressive Strength and Microstructural Characteristics of Natural Zeolite-Based Geopolymer. *Cement and Concrete Composites*, **62**, 64-71.

[3] Dollé, J.B., Agabriel, J., Peyraud, J.L., Faverdin, P., Manneville, V., Raison, C. and Le Gall, A. (2011) Les gaz à effet de serre en élevage bovin: Evaluation et leviers d'action. *INRAE Productions Animales*, **24**, 415-432. https://doi.org/10.20870/productions-animales.2011.24.5.3275

[4] Favier, A. (2013) Mécanisme de prise et rhéologie de liants géopolymères modèles. Master's Thesis, Université Paris-Est, Créteil.

[5] Bouchenafa, O. (2019) Mécanosynthèse et matériaux de construction: Optimisation et application pour la clinkérisation et la géopolymérisation. Master's Thesis, Université Paris-Est, Créteil.

[6] Orsini, S. (2020) Modification des paramètres biotiques et abiotiques du Rizzanes: Impact de l'aménagement hydroélectrique et/ou des conséquence de changement climatique. Master's Thesis, Université de Corse, Corte.

[7] Davidovits, J. (1994) Global Warming Impact on the Cement and Aggregates Industries. *World Resource Review*, **6**, 263-278.

[8] Davidovits, J. (1991) Geopolymers: Inorganic Polymeric New Materials. *Journal of Thermal Analysis and Calorimetry*, **37**, 1633-1656. https://doi.org/10.1007/BF01912193

[9] Cheng, T.W. and Chiu, J.P. (2003) Fire-Resistant Geopolymer Produced by Granulated Blast Furnace Slag. *Minerals Engineering*, **16**, 205-210. https://doi.org/10.1016/S0892-6875(03)00008-6

[10] Bakharev, T. (2005) Resistance of Geopolymer Materials to Acid Attack. *Cement and Concrete Research*, **35**, 658-670. https://doi.org/10.1016/j.cemconres.2004.06.005

[11] Longhi, M.A., Rodriguez, E.D., Walkley, B., Zhang, Z. and Kirchheim, A.P. (2020) Metakaolin-Based Geopolymers: Relation between Formulation, Physicochemical Properties and Efflorescence Formation. *Composites Part B*: *Engineering*, **182**, Article ID: 107671. https://doi.org/10.1016/j.compositesb.2019.107671

[12] Balde, M.Y., Njiomou Djangang, C., Bah, A., Blanchart, P. and Njopwouo, D. (2021) Effect of Physicochemical Characteristics on the Use of Clays from Kindia (Guinea) in Ceramic Compositions. *International Journal of Applied Ceramic Technology*, **18**, 1033-1042. https://doi.org/10.1111/ijac.13669

[13] Balde, M.Y., Djangang, C.N., Diallo, R.B., Blanchart, P. and Njopwouo, D. (2021) Physicochemical Characterisation for Potential Uses as Industrial Mineral of Bauxite from Debele, Guinea. *Journal of Materials Science and Chemical Engineering*, **9**, 9-22. https://doi.org/10.4236/msce.2021.93002

[14] ISO (2018) Standard ISO 5017:2013: Dense Shaped Refractory Products—Determination of Bulk Density, Apparent Porosity and True Porosity. https://www.iso.org/standard/56179.html

[15] Pougnong, T.E., Belibi Belibi, P.D., Baenla, J., Thamer, A., Tiffo, E. and Elimbi, A. (2021) Effects of Chemical Composition of Amorphous Phase on the Reactivity of Phosphoric Acid Activation of Volcanic Ashes. *Journal of Non-Crystalline Solids*, **575**, Article ID: 121213. https://doi.org/10.1016/j.jnoncrysol.2021.121213

[16] Lecomte-Nana, G.L. (2004) Transformations thermiques, organisation structurale et frittage des composés kaolinite-muscovite. Master's Thesis, Université de Limoges, Limoges.

[17] Lecomte-Nana, G.L., Bonnet, J.P. and Blanchart, P. (2011) Investigation of the Sintering Mechanisms of Kaolin-Muscovite. *Applied Clay Science*, **51**, 445-451. https://doi.org/10.1016/j.clay.2011.01.007

[18] Tchakouté, H.K. (2013) Elaboration et caractérisation de ciments géopolymères à base de scories volcaniques. Master's Thesis, Université de Yaoundé I, Yaoundé.

[19] Weng, L., Sagoe-Crentsil, K., Brown, T. and Song, S. (2005) Effects of Aluminates on the Formation of Geopolymers. *Materials Science and Engineering*: *B*, **117**, 163-168. https://doi.org/10.1016/j.mseb.2004.11.008

[20] Elimbi, A., Tchakoute, H.K. and Njopowouo, D. (2011) Effets of Calcination Temperature of Kaolinite Clays on the Properties of Geopolymer Cements. *Construction and Building Materials*, **52**, 2805-2812. https://doi.org/10.1016/j.conbuildmat.2010.12.055

[21] Tchakoute, K.H., Mbey, J.A., Elimbi, A., Diffo Kenne, B.B. and Njopwouo, D. (2013) Synthesis of Volcanic Ash-Based Geopolymer Mortars by Volcanic by Fusion Method: Effect of Adding Metakaolin to Fused Volcanic Ash. *Ceramics International*, **39**, 1613-1621. https://doi.org/10.1016/j.ceramint.2012.08.003

[22] Lecomte, G.L., Bonnet, J.P. and Blanchart, P. (2007) A Study of the Influence of Muscovite on the Thermal Transformations of Kaolinite from Room Temperature up to 1100˚C. *Journal of Materials Science*, **42**, 8745-8752.

https://doi.org/10.1007/s10853-006-0192-7

[23] Djangang, C.N., Mbey, J.A., Ekani, C.J., Tiam, S.T., Blanchart, P. and Njopwouo, D. (2020) Improved Microstructure and Free Efflorescence Geopolymer Binders. *SN Applied Sciences*, **2**, Article No. 2167. https://doi.org/10.1007/s42452-020-03959-6

[24] Jouenne, C.A. (2001) Traité de céramiques et matériaux minéraux. Septima, Paris.

[25] Djangang, C.N. (2007) Argiles kaolinitiques de Mayouom et de Mvan: Caractérisation et utilisation dans l'élaboration des matériaux réfractaires. Master's Thesis, Université de Yaoundé I, Yaoundé.

[26] Yang, T., Chou, C. and Chien, C. (2012) The Effects of Foaming Agents and Modifiers on a Foamed-Geopolymer. *The* 2012 *World Congress on Advances in Civil, Environmental, and Materials Research* (*ACEM*' 12), Seoul, 26-30 August 2012, 905-914.

[27] Tchadjie, N.L. (2012) Comportement thermique des géopolymères obtenus à partir d'une argile kaolinite. Ph.D. Thesis, Université de Yaoundé I, Yaoundé.

[28] Mabah, D.E.T., Tchakouté, H.K., Rüscher, C.H., Kamseu, E., Elimbi, A. and Leonelli, C. (2019) Design of Low Cost Semi-Crystalline Calcium Silicate from Biomass for the Improvement of the Mechanical and Microstructural Properties of Metakaolin-Based Geopolymer Cements. *Materials Chemistry and Physics*, **223**, 98-108. https://doi.org/10.1016/j.matchemphys.2018.10.061

[29] Balde, M.Y. (2023) Physicochemical Characterisation of Aluminosilicates (Clays and Bauxite) from Kindia, Guinea: Application in the Formulation of Hydraulic Mortars and Ceramic Compositions. Revue Francophone. https://www.researchgate.net/publication/374550472_Caracterisation_physicochimique_des_aluminosilicates_argiles_et_bauxite_de_Kindia_Guinee_Application_dans_la_formulation_des_mortiers_hydrauliques_et_des_compositions_ceramique

[30] Yin, S., Yan, Z., Chen, X. and Wang, L. (2022) Effect of Fly-Ash as Fine Aggregate on the Workability and Mechanical Properties of Cemented Paste Backfill. *Case Studies in Construction Materials*, **16**, e01039. https://doi.org/10.1016/j.cscm.2022.e01039

[31] Huang, Y., Huo, Z., Ma, G., Zhang, L., Wang, F. and Zhang, J. (2023) Multi-Objective Optimization of Fly Ash-Slag Based Geopolymer Considering Strength, Cost and CO_2 Emission: A New Framework Based on Tree-Based Ensemble Models and NSGA-II. *Journal of Building Engineering*, **68**, Article ID: 106070. https://doi.org/10.1016/j.jobe.2023.106070

[32] Pratap, B., Sharma, S., Kumari, P. and Raj, S. (2023) Mechanical Properties Prediction of Metakaolin and Fly Ash-Based Geopolymer Concrete Using SVR. *Journal of Building Pathology and Rehabilitation*, **9**, Article No. 1. https://doi.org/10.1007/s41024-023-00360-9